Experimental Mechanics (2023) 63:995–1001
https://doi.org/10.1007/s11340-023-00968-5

RESEARCH PAPER

Experimental Study on Natural Vibration Characteristics of Double-Strip High-Speed Pantograph Head

X. Xu[1] · H. Zhang[1,2] · X. Wei[1] · M. Wu[1] · Z. Zhang[1] · Z. Ye[1] · R. Wu[3] · S. Huang[3]

Received: 16 January 2023 / Accepted: 15 May 2023 / Published online: 26 May 2023

Abstract

Background Pantograph-catenary resonance is one of the main causes of the increased vibration amplitudes of the pantograph-catenary system. Experimental identification of the modal characteristics of the complex mechanics of the pantograph can provide basis for determining whether the pantograph-catenary resonance occurs or not and for modeling pantograph dynamics.

Objective The typical service conditions of the pantograph were simulated, and the modal characteristics of pantograph under different service conditions were identified experimentally.

Methods Modal tests of the DSA380 pantograph were conducted at two working heights of pantograph and three boundary constraints of the pantograph head, and the effects of working heights and boundary constraints on the modal parameters of the pantograph head were studied.

Results The natural frequencies and modal shapes of the DSA380 pantograph head in the frequency range of 200 Hz were identified, including coupling vibration modes associated with the bow spring at 30.35 Hz and below, and elastic modes associated with the elastic deformation of the strip at 34.81 Hz and above.

Conclusions The high-order elastic modes of the strip are related to the material and structural parameters, and has almost nothing to do with the working height of the pantograph and the boundary constraints of the pantograph head, thus only one service condition is needed for future testing. However, the low frequency coupled vibration mode is greatly affected by the operating height and boundary constraints, so it is necessary to conduct modal experiments in specific service conditions.

Keywords Pantograph · Modal characteristics · Working height · Boundary constraint

Introduction

Since Electric Multiple Units (EMUs) obtain electricity from the catenary through the pantograph, a good pantograph-catenary contact is essential for ensuring current collection quality for the high-speed train. With the increase of the running speed of the train, the issue of the pantograph-catenary dynamic characteristics becomes increasingly noticeable. On the one hand, the preliminary design of the dynamic parameters of the pantograph-catenary system and the assessment of the current collection quality of the pantograph-catenary system are usually based on the dynamics modeling and simulation analysis of the pantograph-catenary system, and the consistency of the dynamic behavior of the pantograph model with that of the pantograph-catenary system under the service condition is crucial. On the other hand, pantograph-catenary resonance is one of the main causes of the increased vibration amplitudes of the pantograph-catenary system, which may lead to reduced current collection quality, pantograph-catenary disconnection, or even damage to the pantograph-catenary system. It is particularly important to design the pantograph with natural vibration frequencies that deviate from the frequencies of excitations received by the pantograph-catenary system. Therefore, experimentally identifying the natural vibration characteristics of the pantograph for different service conditions can provide an

✉ X. Xu
xxh@lnm.imech.ac.cn

[1] State Key Laboratory of Nonlinear Mechanics, Institute of Mechanics, Chinese Academy of Sciences, 100190 Beijing, China

[2] School of Engineering Sciences, University of Chinese Academy of Sciences, Beijing 100049, China

[3] Beijing CRRC CED Railway Electric Tech Company Limited, Beijing 100176, China

experimental basis and validation for the dynamics modeling of the pantograph. The identified natural vibration characteristics can be further used for optimization of parameters of the pantograph during preliminary design to avoid pantograph-catenary resonance.

When the train is running at a speed below 320 km/h, the pantograph is mainly excited by the frequency of passing the catenary steady arms and droppers, which will excite the coupled vibration mode of the pantograph below 20 Hz [1–5] and the low-frequency pantograph-catenary dynamics [6, 7]. As the running speed increases, the pantograph is subject to higher excitation frequencies during operation due to catenary irregularity [8–11], wear of strip surface [10], aerodynamic effects [12] and other factors, which will excite the high-frequency elastic mode of the pantograph strip and the high-frequency interaction between the pantograph and catenary [13, 14]. Experimental studies on the correlation between the vertical acceleration spectrum of the pantograph head and the electric arc intensity spectrum below 500 Hz have shown that pantograph-catenary disconnection and electric arc are related to the rigid body motion of the pantograph, as well as the high-frequency dynamic behaviors of the strip [15].

For decades, scholars have been devoted to establishing the dynamic model of the complex mechanics of the pantograph to characterize the coupled dynamic behaviors of the pantograph−catenary system for actual service boundaries. The main pantograph models include: the three-mass model [1, 7, 16, 17] thatreflects the vertically coupled vibration mode of the pantograph, the multi-rigidbody model [18–20] that is focused on thedegrees of motion freedom of the pantograph mechanism, the elastic pantograph head model [13, 21–25]in which the high-order elastic modes of the pantograph strip are considered,the full elastic model [14, 26, 27] in whichthe elastic modes of both the pantograph head and the frame are taken intoaccount, etc. Modal experiments are an effective means to obtain structuraldynamic parameters and validate the dynamic model [5, 28–32].

In modal experiments, a vibration generator or hammer is usually used for excitation, and displacement or acceleration sensors for vibration pick-up. Only the natural frequency of the structure can be measured when there are only a small number of vibration pick-up points, and vibration mode will be lacking in subsequent structural dynamic modeling. If there are enough vibration pick-up points, both the natural frequency and vibration mode of the structure can be measured at the same time. For DSA250 [33], DSA380 [34], TSG [1], HEMU-430X [2] and other unknow types of pantograph [3–5], 1 to 3 vibration pick-up points were arranged in each of the pantograph head or frame or other components, and 1 ~ 3 coupled vibration frequencies within 20 Hz were measured. In a similar way, for the Dozler test pantograph with an aluminum rod in place of the strip and without pantograph head spring, 16 low-frequency coupled vibration frequencies and high-order elastic vibration frequencies below 200 Hz were measured [11]. Further, for the separate pantograph head, two springs were used to support the two ends to simulate suspension, and the experiment identified the high-order elastic natural vibration frequencies and vibration modes of three types of pantograph heads, including the ART95 pantograph head with 7 elastic modes from 60 to 437 Hz, the DSA350S pantograph head with 4 elastic modes from 81 ~ 476 Hz Hz, the CX25 pantograph head with 8 elastic modes from 49 ~ 206 Hz [13].

As a matter of fact, the pantograph head is connected to the frame by the pantograph head spring, and this suspension connection, as well as the rigidity of the pantograph head spring and frame, can affect the coupled vibration of the pantograph head. The modal characteristics obtained from the test pantograph without pantograph head spring or from single pantograph head cannot reflect the dynamic behavior of the complex mechanics. Therefore, it is necessary to obtain the low- and high-frequency modal parameters for boundaries close to the service conditions for actual pantographs through experiment.

The working height of the pantograph ranges from 1100 to 3100 mm and the conventional working height is 1600 mm. The contact and interaction between the catenary and pantograph are equivalent to the boundary constraint at the pantograph head. Specifically, when the pantograph and catenary are disconnected with each other or the contact force between them is small, it approximates to suspension of the pantograph head; when the pantograph is in contact with the catenary, it approximates to constrained boundary of the pantograph head. Moreover, when the pantograph head is in contact with different parts of the catenary such as contact lines and steady arms, it approximates to constrained boundaries with different contact rigidities.

In this paper, modal experiments of the DSA380 pantograph were carried out for the cases of conventional working height of 1600 mm and high working height of 2400 mm, and free and constrained boundaries of the pantograph head. The natural frequency and vibration mode of the pantograph head under five service conditions in the frequency range of 200 Hz were identified, and the effects of working height and pantograph head boundary on the modal parameters of the pantograph head were explored.

Theory of Modal Test and Analysis

Modal tests were conducted on the DSA380 pantograph with the hammer excitation method. During the test, the force hammer was used to strike the pre-defined hammering points, and the acceleration information of the measured points was recorded through the acceleration sensor. The

excitation and response signals were transformed from the time domain to the frequency domain by the fast Fourier transform, and the frequency response function was solved by the input-input power spectrum and the input-output power spectrum. To reduce the experimental error, the accidental error was reduced by hammering N times. The time domain signal of the force for the n-th ($n=1,\ldots,N$) hammering is denoted by $\mathbf{F}_n(t)$, and the time domain signal of the acceleration for the i-th ($i=1, \ldots, I$) vibration pick-up point in a certain direction is denoted by $\mathbf{X}_{ni}(t)$, where I is the number of vibration pick-up points. The corresponding frequency domain signal $\mathbf{F}_n(\omega)$ and $\mathbf{X}_{ni}(\omega)$ was obtained by fast Fourier transform. By the input-output power spectrum $\mathbf{G}_{\mathrm{XF}i} = \sum_{n=1}^{N} \mathbf{X}_{ni}(\omega)\mathbf{F}_n{}^{*}(\omega) \Big/ N$ and the input-input power spectrum, the frequency response function vector $\mathbf{H}_i = \mathbf{G}_{\mathrm{XF}i} \Big/ \mathbf{G}_{\mathrm{FF}}$, where the superscripts * represents the conjugate of the vectors.

An $I\times m$ matrix was formed by paralleling the frequency-response function vectors based on all vibration pick-up points. The PolyMAX [35] modal identification algorithm was used for parameter estimation to obtain parameters such as the natural frequency, vibration mode and damping ratio of the pantograph. Modal Assurance Criterion (MAC) matrix [36] was introduced to assess the spatial intersection angle of the modal vectors.

$$\mathrm{MAC}_{rs} = \frac{\left|\boldsymbol{\Phi}_r{}^{\mathrm{T}}\boldsymbol{\Phi}_s{}^{*}\right|^2}{\left(\boldsymbol{\Phi}_r{}^{\mathrm{T}}\boldsymbol{\Phi}_r{}^{*}\right)\left(\boldsymbol{\Phi}_s{}^{\mathrm{T}}\boldsymbol{\Phi}_s{}^{*}\right)} \tag{1}$$

where MAC_{rs} is the correlation coefficient between the r-th and s-th modal vectors, which located in the r-th row and the s-th column of the matrix; $\boldsymbol{\Phi}_r$ and $\boldsymbol{\Phi}_s$ are the two modal vectors identified from the parameters; the superscripts * and $^{\mathrm{T}}$ represent the conjugate and transpose of the vectors, respectively. If $\boldsymbol{\Phi}_r$ and $\boldsymbol{\Phi}_s$ are the same modal vectors, $\mathrm{MAC}_{rs}=1$. If they are two different physical modal vectors, $\mathrm{MAC}_{rs}=0$, which means the two modal vectors are orthometric and the two vibration modes are mutually independent. Thus MAC_{rs} is between 0 ~ 1, the more independent the two vibration modes the MAC_{rs} is closer to 0, while the more similar the two vibration modes the MAC_{rs} is closer to 1.

Experimental Scheme and Process

The DSA380 pantograph used in the experiment is designed and produced by Beijing CRRC CED Railway Electric Tech. Co., Ltd. The pantograph is a complex mechanics consisting of several components. The pantograph head is connected to the frame by four tension springs, and the connection between the bars of the frame is articulated. Therefore, the pantograph has low vibration transfer efficiency and complex vibration modes.

In actual service, the pantograph base is bolted to the insulator installed on the top of the train, and the pneumatic spring at the base generates a lifting torque to act on the lower arm, which is transmitted through two four-bar mechanisms to raise the pantograph to a given working height to contact the catenary, and the pneumatic spring pressure can be adjusted to make the contact force between the pantograph and catenary reach the target value to achieve stable current collection.

During the experiment, the pantograph base was bolted to the test bench and the difference between the working height and the set value was less than 2 mm by adjusting the pneumatic spring pressure for a given pan head constraint. The modal characteristics of the pantograph under five service conditions was tested by hammer excitation method with a single-point excitation and multi-point vibration pick-up (Fig. 1(a)~(e)). Two working heights of 1600 and 2400 mm were selected to examine both conventional and high modes of operation. Three pantograph head constraining states, i.e. free, flexible and rigid boundaries, were selected to explore the different imposed constraints on the pantograph head during working. For the free boundary, there is no constraint above the strip, and the lifting torque provided by the pneumatic spring is in equilibrium with the torque due to the pantograph's own gravity. For the flexible and rigid boundaries, there is a contact pressure of 80 N at the midpoint of the strip, and the contact rigidities are 100 N/m and 10^6 N/m, respectively, where the lifting torque provided by the pneumatic spring is in equilibrium with the torque due

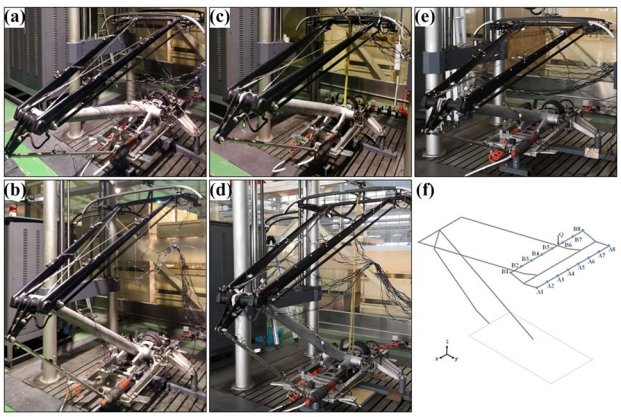

Fig. 1 Photographs of modal test of double-strip high-speed pantograph. Free suspension at working height 1600 mm (**a**) and 2400 mm (**b**), respectively; flexible boundary at working height 1600 mm (**c**) and 2400 mm (**d**), respectively; rigid boundary at working height 1600 mm (**e**). And schematic diagram of excitation point and measure points (**f**), arrow Q indicates the hammer point, No.A1 ~ No.A8 and No.B1 ~ No.B8 indicate the positions of the measure points

to both the pantograph's own gravity and the torque due to the contact pressure.

The test system consisted of DH5902N 32-channel high-speed data acquisition instrument, 1A302E three-way acceleration sensor, hammer with maximum load range of 60 kN, and DHDAS test analysis software. Considering that the mass of the sensors might influence the vibration mode of the structure, a group measurement method was used and the sensors arranged in groups at the measurement points of each component. Eight sensors were arranged evenly on each strip and two strips for a total of 16 measurement points, which were tested in two groups (Fig. 1(f)). Hammering excitation was carried out between two measurement points in turn. By comparing and analyzing the frequency response curves of each measurement point corresponding to different hammering points, the mid-point between B5 and B6 was determined as the hammering point for the pantograph head modal test, where the vibration could be excited in a suitable frequency range and transmitted to all measurement points. In addition, 18, 4, 9 and 7 measurement points were placed at the upper arm, cross arm, lower arm and lower rod, respectively, and the test was divided into four groups to assist in the mode identification of the pantograph head vibration modes.

Experimental Data Analysis

Based on the experimentally measured frequency response curves, the modal parameters of the DSA380 pantograph head below 200 Hz were obtained by using the PolyMAX modal identification algorithm. Figure 2 shows the correlation coefficient MAC_{rs} of the r-th and s-th modal vectors under the five service conditions, including free boundary at working height of 1600 and 2400 mm, flexible boundary at working height of 1600 and 2400 mm, and rigid boundary at working height of 1600 mm. The color and size of the points in the figure indicate the value of MAC_{rs}, that is, the larger the size, the larger the value of MAC_{rs}. According to the statistics of all MAC_{rs}, it can be noted that the correlation coefficients between the modal vectors of different modes range from 0 to 0.4, with 96.26% of the correlation coefficients less than 0.25 and 87.62% of the correlation coefficients less than 0.1. In other words, the modal vectors of different modes obtained in this paper are independent of each other.

Figure 3 presents the frequency response curves of the DSA380 pantograph head under the five service conditions. The vertical dotted line positions correspond to the natural vibration frequencies, and the corresponding vibration mode numbers are marked. Among them, thick solid lines, thin solid lines, dashed lines and dotted lines represent the sum of the frequency response functions in the three directions, as well as

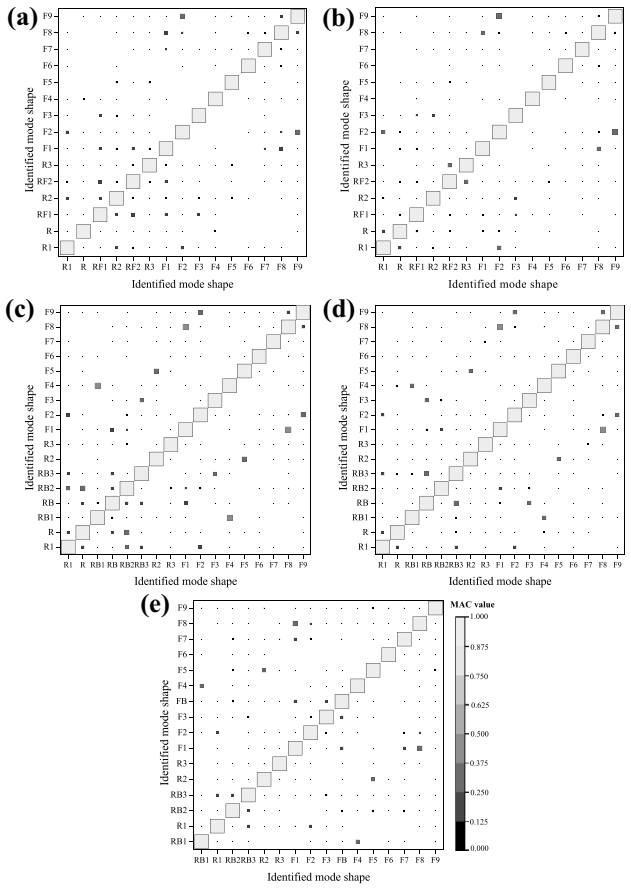

Fig. 2 MAC. Free suspension at working height 1600 mm (**a**) and 2400 mm (**b**), respectively; flexible boundary at working height 1600 mm (**c**) and 2400 mm (**d**), respectively; rigid boundary at working height 1600 mm (**e**)

in the x, y and z, respectively. Figure 4 illustrates some of the vibration modes of the DSA380 pantograph head.

Coupled Vibration Modes

Pitching motion of the pan head R1 (Fig. 4(a)), cross side rolling of the two strips R2 (Fig. 4(b)) and three-axis slip of the two strips R3 (Fig. 4(c)) were 3 coupled vibration modes that occurred successively under all five service conditions. In which:

1. The modal frequency of R1 was related to the working height of the pantograph and the pan head constraint. When the working height was 1600 mm, the modal frequency was 4.50 Hz for the free boundary, 1.59 Hz higher than that for the flexible boundary, and 3.08 Hz lower than that for the rigid boundary; when the working height was 2400 mm, the modal frequency was 3.88 Hz for the free boundary and 0.90 Hz higher than that for

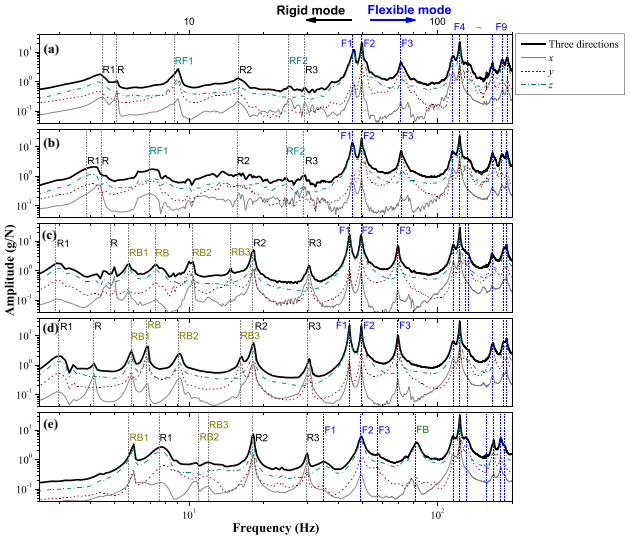

Fig. 3 Frequency response function curves of the collectors. Free suspension at working height 1600 mm (**a**) and 2400 mm (**b**), respectively; flexible boundary at working height 1600 mm (**c**) and 2400 mm (**d**), respectively; rigid boundary at working height 1600 mm (**e**)

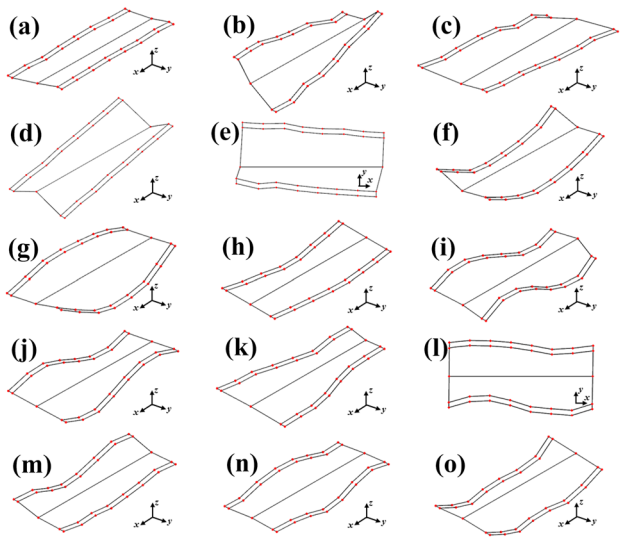

Fig. 4 Mode shapes of the DSA380 pantograph head. (**a**) Pitching motion of the pan head R1; (**b**) Cross side rolling of the two strips R2; (**c**) Three-axis slip of the two strips R3; (**d**) Side rolling of the pan-head RB1; (**e**) Swing in xy plane ofthe pan head RB2; (**f**) Vertical 1st bending vibration of the pan head F1; (**g**) Vertical 1st reversed bending vibration of the two strips F2; (**h**) Longitudinal 1st bending vibration of the pan head F3; (**i**) Vertical 2nd bending vibration of the pan head F4; (**j**) Vertical 2nd reversed bending vibration of the two strips F5; (**k**) Longitudinal 2nd reversed bending vibration of the two strips F6; (**l**) Longitudinal 2nd bending vibration of the pan head F7; (**m**) Vertical 3rd bending vibration of the pan head F8; (**n**) Vertical 3rd reversed bending vibration of the two strips F9; (**o**) Vertical 1st bending vibration of the pan head (the displacementat both ends is 0) FB

the flexible boundary. When the pan head constraint was the free boundary, the modal frequency at the working height of 2400 mm was 0.62 Hz lower than that at 1600 mm; when the pan head constraint was the flexible boundary, the modal frequencies at the two working heights were almost equal.

2. The modal frequency of R2 was related to the pan head constraint and almost independent of the working height. The modal frequency under the two service conditions for the free boundary was approximately 15.73 ± 0.12 Hz, and the modal frequency under the three service conditions for the flexible and rigid boundaries was approximately 18.05 ± 0.01 Hz, which was 2.32 Hz higher than that for the free boundary.
3. The modal frequency of R3 was independent of the working height and the pan head constraint. The modal frequency under the five service conditions was 29.67 ± 0.60 Hz.

The transverse vibration of pan head R was the coupled vibration mode occurring under the four service conditions for the free and flexible boundaries, with a modal frequency of 4.62±0.43 Hz. This mode was not present under this condition due to the large vertical contact rigidity of the rigid boundary, which limited the transverse vibration of the pan head.

The three-way vibrations of pantograph head RF1 and RF2 were coupled vibration modes that occurred successively under the two service conditions for the free boundary, with modal frequencies of 7.84±1.27 Hz and 24.94±0.46 Hz, respectively. Both the modal frequencies decreased slightly when the working height increased. The three service conditions corresponding to the flexible or rigid boundary did not have the two vibration modes, due to the constraint limit on the flexible or rigid boundary.

Side rolling of the pan head RB1 (Fig. 4(d)), swing in xy plane of the pan head RB2 (Fig. 4(e)) and longitudinal vibration of the pan head RB3 were 3 coupled vibration modes that occurred successively under the three service conditions for the flexible or rigid boundaries, but the two service conditions corresponding to the free boundary did not have these three modes. In which:

1. The modal frequency of RB1 was independent of the working height of the pantograph or the boundary constraint vertical rigidity, with a modal frequency of 5.75±0.08 Hz.
2. The modal frequency of RB2 was independent of the vertical rigidity of the boundary. When the working height was 1600 mm, the modal frequency under the two service conditions for the flexible or rigid boundary was 10.63±0.47 Hz; however, the modal frequency of

RB2 for the flexible boundary was related to the working height of the pantograph, and the modal frequency decreased slightly when the working height increased.
3. The modal frequency of RB3 was related to the working height of the pantograph and the vertical rigidity of the boundary. The modal frequency at the working height of 1600 mm for the flexible boundary was 14.72 Hz. The modal frequency for the flexible boundary increased when the working height increased. The modal frequency for the rigid boundary decreased when the working height remained unchanged and the vertical rigidity of the boundary increased.

The pan head's longitudinal vibration RB was a coupled vibration mode occurred under two service conditions for the flexible boundary, which was absent for both the free and rigid boundaries. When the working height was 1600 mm, the modal frequency of RB was 7.31 Hz. The modal frequency decreased slightly when the working height increased.

Elastic Mode

Vertical 1st bending vibration of the pan head (Fig. 4(f)), vertical 1st reversed bending vibration of the two strips F2 (Fig. 4(g)), longitudinal 1st bending vibration of the pan head F3 (Fig. 4(h)), vertical 2nd bending vibration of the pan head F4 (Fig. 4(i)), vertical 2nd reversed bending vibration of the two strips F5 (Fig. 4(j)), longitudinal 2nd reversed bending vibration of the two strips F6 (Fig. 4(k)), longitudinal 2nd bending vibration of the pan head F7 (Fig. 4(l)), vertical 3rd bending vibration of the pan head F8 (Fig. 4(m)), and vertical 3rd reversed bending vibration of the two strips F9 (Fig. 4(n)) were the 9 elastic modes that occurred successively under all five service conditions. In which:

1. The modal frequencies of F2 and F4 ~ F9 were independent of the working height of the pantograph and the pan head constraint, and their modal frequencies were 49.38±0.17 Hz, 115.72±0.22 Hz, 122.99±0.11 Hz, 132.23±1.18 Hz, 166.85±0.98 Hz, 182.74±1.92 Hz and 189.62±1.72 Hz, respectively.
2. The modal frequencies of F1 and F3 were independent of the working height and pan head constraint when the boundary constraint rigidity was small. For the four service conditions with the free and flexible boundaries, the modal frequencies of F1 and F3 were 44.77±0.71 Hz and 70.27±1.27 Hz, respectively. However, for the rigid boundaries with large vertical constraint rigidity, the 2 modal frequencies decreased significantly to 34.81 and 57.50 Hz, respectively.

In addition, vertical 1st bending vibration of the pan head FB was an elastic mode unique to the rigid boundary constraint, with a modal frequency of 81.67 Hz. The displacement at both ends of the strip for this vibration mode was 0, while the displacement at both ends of the strip for F1 was extremely large.

Conclusions

In this paper, the actual service conditions of the high-speed pantograph were experimentally simulated, at two working heights of 1600 and 2400 mm, corresponding to conventional operation and high-catenary operation, respectively; there were three types of boundary constraints: free suspension, flexible constraint and rigid constraint applied at the pantograph head. The three types of boundary constraints respectively correspond to pantograph-catenary disconnection or contact with low contact force, the pantograph head contacting the catenary with a low vertical rigidity, and the pantograph head contacting catenary steady arms with a high vertical rigidity. Modal tests on the DSA380 pantograph in service were conducted to identify the natural frequencies and vibration modes of the pan head below 200 Hz, including coupled vibration modes associated with the bow spring at 30.35 Hz and below, and elastic modes associated with the flexible deformation of the strip at 34.81 Hz and above. On the one hand, the higher-order elastic modes of the strip are related to the material and structural parameters and almost independent of the working height of the pantograph and the boundary constraint of the pan head, thus only one service condition are required in future modal test, such as the most common working condition reported in the present, the working height of 1600 mm and the free suspension constraint of the pan head. On the other hand, the low-frequency coupled vibration modes are more influenced by the working height and the boundary constraint, and thus modal tests are required for specific service conditions.

Acknowledgements This work has been sponsored by National Natural Science Foundation of China (11672297).

Data Availability Data available on request from the authors.

Declarations

Conflict of Interest The authors declare that they have no conflict of interest.

References

1. Zhou N, Zhang WH (2010) Investigation on dynamic performance and parameter optimization design of pantograph and catenary system. Finite Elem Anal Des 47(3):288–295
2. Lee JH, Park TW, Oh HK, Kim YG (2015) Analysis of dynamic interaction between catenary and pantograph with experimental verification and performance evaluation in new high-speed line. Veh Syst Dyn 53(8):1117–1134

3. Ambrósio J, Pombo J, Pereira M (2013) Optimization of high-speed railway pantographs for improving pantograph-catenary contact. Theor Appl Mech Lett 3(1):013006
4. Vieira R (2016) High Speed Train Pantograph Models Identification. Dissertation, University of Lisbon
5. Zhu M, Zhang SY, Jiang JZ, Macdonald J, Neild S, Antunes P, Pombo J, Cullingford S, Askill M, Fielder S (2021) Enhancing pantograph-catenary dynamic performance using an inertance-integrated damping system. Veh Syst Dyn 60(6):1909–1932
6. EN 50317 (2012) Railway applications-current collection systems-requirements for and validation of measurements of the dynamic interaction between pantograph and overhead contact line, European Committee for Electrotechnical
7. EN 50318 (2018) Railway applications-current collection systems-validation of simulation of the dynamic interaction between pantograph and overhead contact line, European Committee for Electrotechnical
8. Zhang WH, Mei GM, Zeng J (2002) A study of pantograph/catenary system dynamics with influence of presag and irregularity of contact wire. Veh Syst Dyn 37:593–604
9. Van Olivier V, Massat J-P, Laurent C, Balmès E (2013) Introduction of variability into pantograph–catenary dynamic simulations. Vehicle Syst Dyn 52(10):1254–1269
10. Song DL, Jiang YA, Zhang WH (2016) Dynamic performance of a pantograph-catenary system with consideration of the contact surface. Proc Inst Mech Eng F J Rail 232(1):262–274
11. Nåvik P, Derosa S, Rønnquist A (2020) On the use of experimental modal analysis for system identification of a railway pantograph. Int J Rail Transp 9(2):132–143
12. Bocciolone M, Resta F, Rocchi D, Tosi A, Collina A (2006) Pantograph aerodynamic effects on the pantograph-catenary interaction. Veh Syst Dyn 44(sup1):560–570
13. Collina A, Lo Conte A, Carnevale M (2009) Effect of collector deformable modes in pantograph-catenary dynamic interaction. Proc Inst Mech Eng F J Rail 223(1):1–14
14. Ambrósio J, Rauter F, Pombo J, Pereira MS (2011) A flexible multibody pantograph model for the analysis of the catenary-pantograph contact. ECCOMAS Thematic Conference on Multibody Dynamics, Warsaw Univ Technol, Warsaw, Poland
15. Collina A, Melzi S (2006) Effect of contact strip-contact wire interaction on current transfer at high sliding speed in the mid-high frequency range. AITC-AIT International Conference on Tribology Parma, Italy
16. Eppinger SD, O'Connor DN, Seering WP, Wormley DN (1988) Modeling and experimental evaluation of asymmetric pantograph dynamics. J Dyn Syst T Asme 110(2):168–174
17. Bruni S, Ambrosio J, Carnicero A, Cho YH, Finner L, Ikeda M, Kwon S, Massat J, Stichel S, Tur M, Zhang WH (2014) The results of the pantograph-catenary interaction benchmark. Veh Syst Dyn 53(3):412–435
18. Massat J-P, Laurent C, Bianchi J-P, Balmès E (2014) Pantograph catenary dynamic optimisation based on advanced multibody and finite element co-simulation tools. Veh Syst Dyn 52(sup1):338–354
19. Bautista A, Montesinos J, Pintado P (2016) Dynamic interaction between pantograph and rigid overhead lines using a coupled FEM multibody procedure. Mech Mach Theory 97:100–111
20. Yao YM, Zhou N, Zou D, Mei GM, Zhang WH (2020) Collision dynamics analysis of lifting the pantograph. Proc Inst Mech Eng F J Rail Rapid 235(4):450–462
21. Liu ZD, Jönsson P, Stichel S, Rønnquist A (2014) Implications of the operation of multiple pantographs on the soft catenary systems in Sweden. Proc Inst Mech Eng F J Rail 230(3):971–983
22. Zhou N, Zhang WH, Li RP (2018) Dynamic performance of a pantograph-catenary system with the consideration of the appearance characteristics of contact surfaces. J Zhejiang Univ Sci A 12(12):467–480
23. Zhou N, Zou H, Li RP, Mei GM, Zhang WH (2016) Dynamic behavior of different pantograph models in simulation of pantograph and catenary interaction. 35th Chinese Control Conference Chengdu, Sichuan, China
24. Collina A, Bruni S (2002) Numerical simulation of pantograph-overhead equipment interaction. Veh Syst Dyn 38:261–291
25. Tuissi A, Bassani P, Casati R, Bocciolone M, Collina A, Carnevale M, Lo Conte A, Previtali B (2009) Application of SMA composites in the collectors of the railway pantograph for the italian high-speed train. J Mater Eng Perform 18(5–6):612–619
26. Massat J, Laurent C, Bianchi J, Balmes E (2014) Pantograph catenary dynamic optimisation based on advanced multibody and finite element co-simulation tools. Exp Mech 52:338–354
27. Szeląg A, Wilk A, Judek S, Karwowski K, Mizan M, Kaczmarek P, Karwowski K, GoldH, Żurkowski A (2018) Modal analysis of railway current collectors using Autodesk Inventor. MATEC Web of Conferences Warsaw, Poland
28. [Canada2022a], Agrawal P, Salehian A (2022) Dynamic analysis and experimental validation of periodically wrapped cable-harnessed plate structures. Exp Mech 62(6):909–927
29. [Italy2021a], Briccola D, Cuni M, De Juli A, Ortiz M, Pandolfi A (2020) Experimental validation of the attenuation properties in the sonic range of metaconcrete containing two types of resonant inclusions. Exp Mech 61(3):515–532
30. Doan N, Le V, Park H, Goo N (2022) Modal analysis using a virtual speckle pattern based digital image correlation method: an application for an artificial flapping wing. Exp Mech 62(2):253–270
31. [Turkey2022a], Karaağaçlı T, Özgüven HN (2021) Experimental quantification and validation of modal properties of geometrically nonlinear structures by using response-controlled stepped-sine testing. Exp Mech 62(2):199–211
32. Koyuncu A, Karaağaçlı T, Şahin M, Özgüven HN (2022) Experimental modal analysis of nonlinear amplified piezoelectric actuators by using response-controlled stepped-sine testing. Exp Mech 62(9):1579–1594
33. Li DY, Wu JQ, Guan JF (2012) Simulation and test of vibration characteristics of DSA250 pantograph. Electr Railway 23(4):7–10 (in Chinese)
34. Gao WB, Ma GL, Ma SQ, Li JT, Fang J (2015) Study on the pantograph modal test of type DSA380 for high-speed train. J Dalian Jiaotong Univ 36(6):24–28 (in Chinese)
35. Peeters B, Van der Auweraer H, Guillaume P, Leuridan J (2004) The PolyMAX frequency-domain method: a new standard for modal parameter estimation? Shock Vib 11(3–4):395–409
36. Allemang RJ (1980) Investigation of some multiple input/output frequency response function experimental modal analysis techniques. Dissertation, University of Cincinnati